

1 The Liquid Argon Purity Demonstrator

2 M. Adamowski^a, B. Carls^a, E. Dvorak^b, A. Hahn^a, W. Jaskierny^a, C. Johnson^a, H. Jostlein^a,
3 C. Kendziora^a, S. Lockwitz^a, B. Pahlka^{a*}, R. Plunkett^a, S. Pordes^a, B. Rebel^a, R. Schmitt^a,
4 M. Stancari^a, T. Tope^{a†}, T. Yang^a

5 ^aFermi National Accelerator Laboratory, P.O. Box 500, Batavia, IL, 60510, USA

6 ^bSouth Dakota School of Mines & Technology, 501 East Saint Joseph Street, Rapid City, SD
7 57701

8 **Contents**

9	1 Introduction	2
10	1.1 TPC Introduction	2
11	1.2 Previous Work	2
12	1.3 The Liquid Argon Purity Demonstrator	3
13	2 The Cryostat	4
14	3 The Cryogenics	7
15	3.1 Phase Separator and Condenser	7
16	3.2 Filters	7
17	3.3 Piping and Valves	10
18	3.4 Recirculation Pump	10
19	3.5 Control System	12
20	4 Cryostat Instrumentation	12
21	4.1 RTD Translators	12
22	4.2 Purity Monitors	16
23	4.2.1 Hardware	16
24	4.2.2 Data Acquisition	18
25	4.2.3 Fiber Quality checks	21
26	4.2.4 Systematic Uncertainties	22
27	4.3 Gas Analyzers	23
28	4.3.1 Oxygen, Water and Nitrogen Monitors	23
29	4.3.2 Oxygen Capillary Detectors	23
30	5 Results from Operation Modes	24
31	5.1 Gaseous Argon Purge	25
32	5.2 Gas Recirculation	26
33	5.3 Liquid Argon Filling	26

*Corresponding author: pahlka@fnal.gov (B. Pahlka)

†Corresponding author: tope@fnal.gov (T. Tope)

1	5.4 Liquid Argon Recirculation	28
---	--	----

2	6 Discussion and Conclusion	31
---	------------------------------------	-----------

3 **ABSTRACT** We report on measurements of the electron drift lifetime in the liquid argon and
 4 the associated measurements (contaminant concentrations and temperature) using the Liquid
 5 Argon Purity Demonstrator. We describe the apparatus, operational phases, and critical devices.
 6 The results show that long electron lifetimes can be achieved without initial cryostat evacuation,
 7 which is of particular interest in designing large liquid argon TPCs.

8 **1. Introduction**

9 **1.1. TPC Introduction**

10 Liquid argon (LAr) time projection chambers (TPCs) provide a robust and elegant method
 11 for measuring the properties of charged particle interactions by providing 3D event imaging with
 12 excellent spatial resolution. The ionization electrons created by the passage of charged particles
 13 through the liquid can be transported without distorting information about the location of
 14 ionization by a uniform electric field over macroscopic distances. Imaging is typically facilitated
 15 by three sets of parallel wires, oriented with different directions and placed at the end of the drift
 16 path. The wires continuously propagate the signals induced by the drifting electrons which are
 17 then recorded by electronics. This technology relies on drifting ionization electrons from the site
 18 of energy deposition to readout wires up to two meters or more away without interaction with
 19 electronegative contaminants and has been employed successfully in both neutrino and dark
 20 matter experiments[REFS?]. LArTPC technology has experienced renewed and strengthened
 21 interest since having recently been chosen as the preferred technology for a future long-baseline
 22 neutrino oscillation experiment [1].

23 **1.2. Previous Work**

24 The ICARUS Collaboration led a pioneering effort in the research and development of LAr
 25 TPC technology for the past 25 years. The T600 LArTPC is housed in a 760 ton cryostat.
 26 This cryostat is surrounded by insulating layers of Nomex honeycomb cells [2]. The volume
 27 of the cryostat was **baked out** under vacuum to 10^{-4} mbar before filling. Electron lifetimes
 28 greater than 6 ms were obtained with a contamination less than 0.1 parts per billion (ppb)
 29 water equivalent [3].

30 The Materials Test Stand (MTS) at the Fermi National Accelerator Laboratory (Fermilab)
 31 was developed to evaluate the effect of different materials on electron lifetime [4]. The system
 32 used a 250 L vacuum-insulated vessel that was evacuated before filling to a pressure of 10^{-6} Torr.
 33 The system purified commercial argon using filters similar to those described in Section 3.2**need**
 34 **brief description here**. The MTS recorded electron lifetimes not in excess of 8 ms with a purity
 35 monitor similar to those detailed in Section 4.2.

36 Later at Fermilab, the ArgoNeuT project was the first LAr TPC in The United States to be
 37 placed in a neutrino beam [6]. Commissioned in 2009, it had an 550 L vacuum insulated cryostat
 38 that was evacuated before filling with LAr. The purification system only purified reliquefied
 39 argon gas boiled-off in the gaseous region of the cryostat. With this system, ArgoNeuT was able
 40 to obtain lifetimes of about 750 μ s.

41 The ARGONTUBE LArTPC of AEC-LHEP University of Bern was developed to investigate
 42 the ability to drift electrons over distances of up to 5 m [7]. It uses a vacuum insulated cryostat
 43 and is evacuated to 5×10^{-5} mbar before filling with LAr. ARGONTUBE has been able to
 44 reach contamination levels down to 1 part per million (ppm) and achieve lifetimes of 2 ms with
 1 a 240 V/cm drift field **check with T. Strauss**.

2 The conventional liquid argon vessels described in this section are evacuated to remove water,
 3 oxygen, and nitrogen contaminants present in the ambient air prior to filling with liquid argon.
 4 However, as physics requirements dictate larger cryogenic vessels to hold bigger detectors, the
 5 mechanical strength required to resist the external pressure of evacuation becomes prohibitively
 6 costly.

7 1.3. The Liquid Argon Purity Demonstrator

8 The Liquid Argon Purity Demonstrator (LAPD) located at Fermilab is designed to achieve the
 9 ultra high purity required by LArTPCs in a vessel that cannot be evacuated. The purification
 10 of the volume proceeded in three stages to obtain electron lifetimes on the order of several
 11 milliseconds. The system relies heavily on the experience from the MTS at Fermilab [4] in its
 12 design and operation plan. Prior to filling with liquid argon, the ambient air is removed by
 13 purging the tank with argon gas. It has been shown that the concentration of oxygen in a
 14 vessel purged with gaseous argon can be reduced to 100 ppm after 2.6 volume exchanges [5].
 15 After the initial purge, the walls of the cryostat were heated to dry the surfaces of the vessel.
 16 Once the water and oxygen concentrations are at the level of ppm, the gas is subsequently
 17 circulated through filter vessels to further reduce these contaminants. Finally, liquid argon is
 18 then introduced into the vessel after a concentration of impurities less than 1 parts-per-million
 19 (ppm) is achieved. The liquid is continuously circulated through the filter vessels in order
 20 to achieve concentrations of water and oxygen on the order of 0.1 parts-per-billion (ppb). A
 21 photograph of the LAPD vessel is shown in Figure 1.

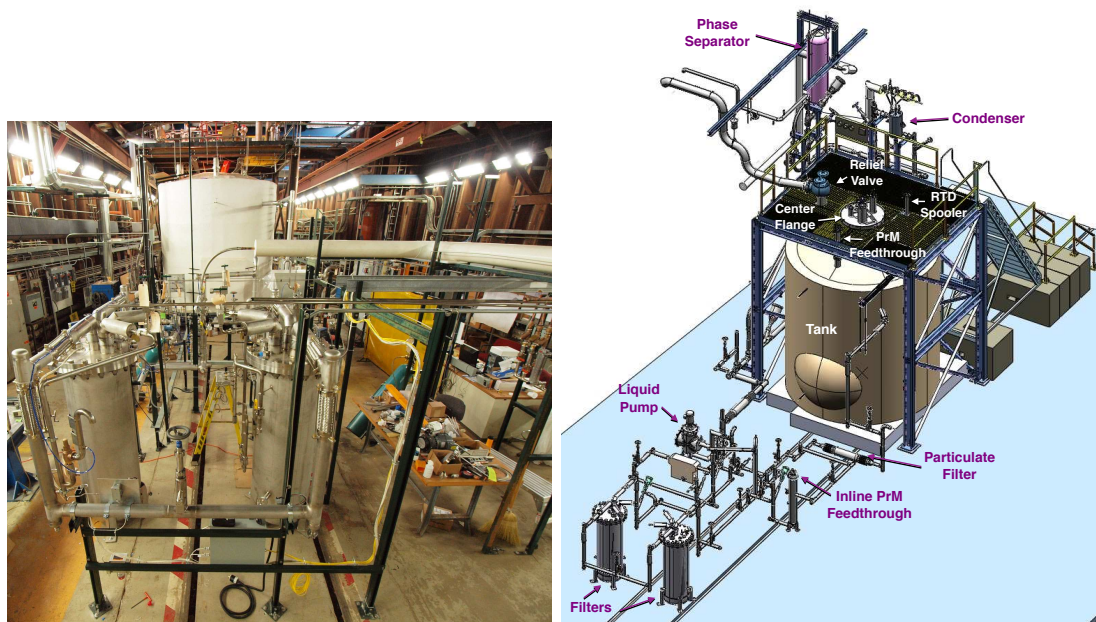


Figure 1. A photograph of the Liquid Argon Purity Demonstration (LAPD) at Fermilab (left) and 3D model of the system (right).

1 in the bulk liquid and concentrations of water and oxygen in order to check our models for
2 the behavior of the liquid. Second, we studied the number of liquid argon volume exchanges
3 necessary to achieve drift distances on the scale of 2.5 meters. Third, the filter capacity as
4 a function of flow rate was closely monitored and its performance evaluated. Finally, after
5 achieving the required electron drift lifetimes, the LAPD was emptied and a TPC of 2 m drift
6 distance was placed in the volume. High LAr purity was achieved with the TPC in the tank.
7 The details of the TPC and its performance will be discussed in a separate paper.

8 This document is outlined as follows. The LAPD vessel is described in Section 2. The
9 cryogenics, including the filters and cryogenic valves, are detailed in Section 3. Section 4 dis-
10 cusses the instrumentation to monitor the LAr including the purity monitors, gas analyzers, and
11 temperature-monitoring devices. Finally, Sections 5 and 6 conclude with the results and a brief
12 discussion.

13 2. The Cryostat

14 The LAPD cryostat is an industrial low pressure storage tank. The cryostat has a flat bottom,
15 cylindrical sides, and a dished head. The cryostat diameter is 10 feet and the cylindrical walls
16 have a 10-foot height. The cryostat is fabricated from 3/16 inch-thick SA-240 stainless steel. The
17 internal and external (vacuum) maximum allowable working pressures are 3 psig and 0.2 psig,
18 respectively. Eight perimeter anchors tie the cryostat bottom to the ground to prevent cryostat
19 uplift. The cryostat volume is 6506 gallons of which 5603 gallons is liquid (32.6 tons) with a
20 corresponding liquid depth of 2.9 m. Fabrication followed The American Petroleum Institute
21 Standard 620 Appendix Q as closely as possible. The cryostat welds were fully radiographed.
22 The cryostat is located inside the Proton Center 4 (PC4) building at Fermilab. Figure 2 shows
23 a picture of the LAPD cryostat.

24 The head of the cryostat is populated with four ConFlat flanges and a 30 inch diameter
25 center flange sealed with an indium wire. Metallic seals are used to prevent the diffusion of
26 contamination that would occur through non-metallic seals. The center flange allows for cryostat
27 entry using an extension ladder. Five ConFlat flanges populate the center flange, each of which
28 sit atop stainless steel tube risers such that the ConFlats remain at room temperature when
29 the cryostat is cold. Figure 3 shows the top of the cryostat layout. At ground level a 30 inch
30 diameter welded manhole is available and intended to make access easier for extended work
31 inside the cryostat.

32 **Table X, not yet created, lists the cryostat operating parameters including the heat leak,**
33 **volume, operating pressure, and nominal pump flow rates.**

34 The cryostat sides and top are insulated with 10 inches of fiberglass which is covered by an
35 outer layer of 3/4 inch-thick foam. The foam is covered with glass cloth and a mastic which
36 provides a vapor barrier. The cryostat sits on an insulating structural foam base also sealed
37 with a mastic vapor barrier. The cryostat heat leak is estimated as 2103 W ($X \text{ W/m}^3$). The
38 foam base sits atop two rail cars and cribbing. Natural air flow under the rail cars and cribbing
39 eliminates the need for foundation heaters.

40 The cryostat was cleaned with deionized water and detergent then dried with lint free rags
41 by the cryostat fabricator prior to shipment to Fermilab. After installation of all components
42 at Fermilab the cryostat was vacuumed with a HEPA filter equipped vacuum. After vacuum
43 cleaning, all walls were wiped with deionized water and lint free rags. Stubborn residue was
44 spot removed with alcohol and lint free rags.



Figure 2. LAPD cryostat sitting on an insulating structural foam base in PC4. Insulating foam was added to the sides and head later.

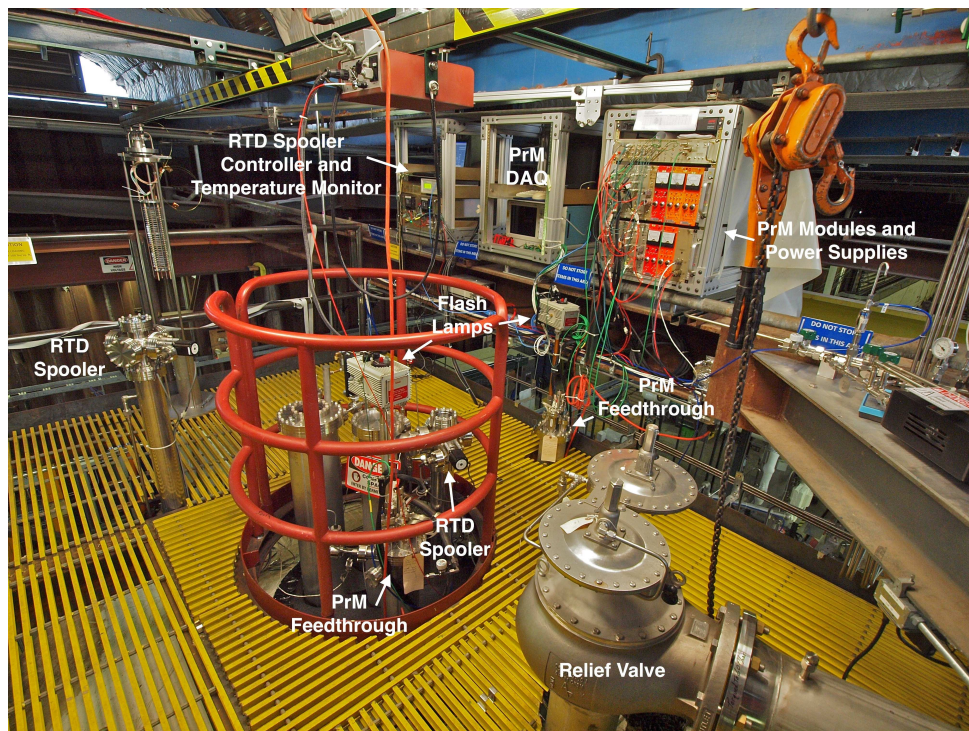


Figure 3. A photograph of the platform on top of the cryostat. The purity monitor feedthroughs, RTD spoolers, and the control systems are shown. [reference sections!](#)

45 3. The Cryogenics

1 3.1. Phase Separator and Condenser

2 The argon vapor generated by ambient heat input is condensed using liquid nitrogen. A 4,000
3 gallon trailer supplies liquid nitrogen through foam insulated 1 inch Type K copper piping. A
4 phase separator operating at 15 psig near the LAPD cryostat vents nitrogen vapor generated
5 in the nitrogen transfer line so that the condenser is supplied with single phase liquid nitrogen.
6 The phase separator and condenser were designed at Fermilab. A control valve feeding the phase
7 separator maintains a constant liquid level in the phase separator. The condenser consists of
8 an argon volume containing three differently sized coils of tubing through which liquid nitrogen
9 flows. The coiled nitrogen tubing is seamless and all nitrogen connections and welds are outside
10 the condenser to mitigate any nitrogen leak into the LAPD cryostat. Argon vapor generated by
11 ambient heat input into the LAPD cryostat is condensed by the liquid nitrogen flowing through
12 the coils.

13 By default, the condensed liquid argon returns to the liquid recirculation pump suction and
14 then goes through the filters during liquid recirculation. This is important since the water
15 outgassing from tank wall above the liquid is mixed with the argon vapor and needs to be
16 removed to maintain good LAr purity. When the pump is off, the condensed liquid argon returns
17 directly to the tank. A control valve feeds the condenser and adjusts the flow to maintain a
18 constant vapor pressure in the ullage. Solenoid valves choose which coil or which combinations
19 of coils receives liquid nitrogen. The calculated cooling capacity of the condenser is 8400 W
20 (reference, put in operating parameters table). The coils operate at near ambient pressure due
21 to the pressure drop across the inlet control valve. They therefore must be covered in a thin layer
22 of argon ice to achieve the required temperature gradient. No noticeable impact on the cooling
23 due to the argon ice was observed. The vaporized nitrogen is vented outside the enclosure and
24 not recovered. Figure 4 showers the sketch of the condenser designed and Figure 5 shows a
25 photo of the phase separator and condenser in PC4.

26 3.2. Filters

27 The purification system contains two filters which have identically sized filtration beds of 77
28 liters. The first filter that the process stream enters contains a 4A molecular sieve supplied
29 by Sigma Aldrich (reference). The 4A molecular sieve primarily removes water contamination
30 but can also remove small mounts of nitrogen and oxygen. The second filter contains BASF
31 CU-0226 S, a highly dispersed copper oxide impregnated on a high surface area alumina to
32 remove oxygen(reference). The oxygen filter also removes water. Thus, the oxygen filter is
33 placed downstream of th molecular sieve to maximize oxygen filtration. The filters are insulated
34 with vacuum jackets and aluminum radiation shields. Metallic radiation shields were chosen
35 because the filter regeneration temperatures would damage traditional aluminized mylar insu-
36 lation. Piping supplying the filter regeneration gas is insulated both inside the filter vacuum
37 insulation space and outside the filter with Pyrogel XT which is an aerogel based insulation
38 (reference) which can withstand temperatures up to 1200 F. Figure 6 shows the 3D model of
39 the filter vessel.

40 The filters are regenerated in place using heated gas. Both filters are regenerated using a
41 flow of argon gas heated to 200 C. The argon gas is supplied by commercial 180 liter liquid
42 argon dewars. Once at 200 C, a small flow of hydrogen is mixed into the primary argon flow.
43 The hydrogen combines with oxygen captured by the filter and creates water. The hydrogen
44 fraction does not exceed 2.5% of the heated gas mixture because the regeneration reaction is
45 exothermic and too much hydrogen causes excess temperatures that damage the filter. The
46 damage is induced by sintering of the copper and greatly reducing the available filter surface

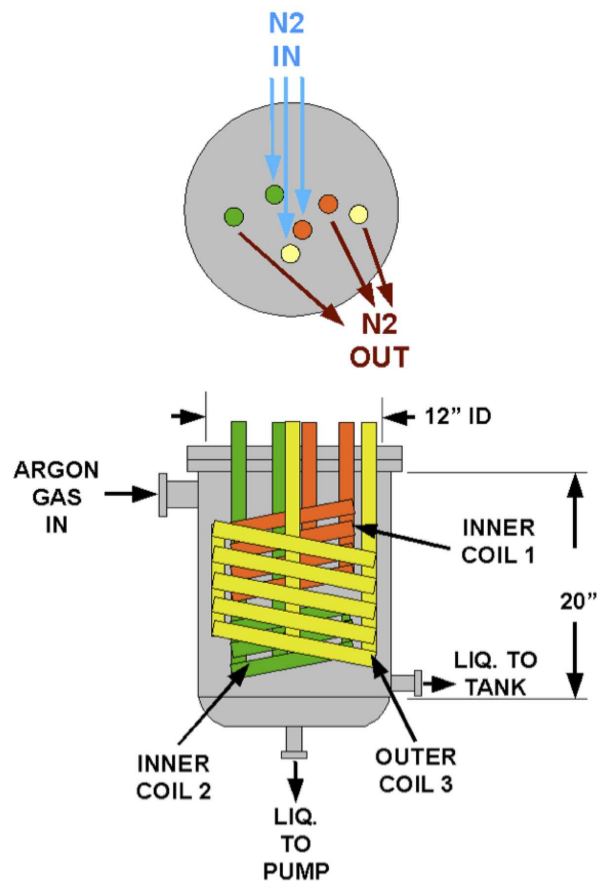


Figure 4. A sketch of the LAPD condenser which shows the three coils of tubing for liquid nitrogen, the inlet for gaseous argon and two outlets for liquefied argon.

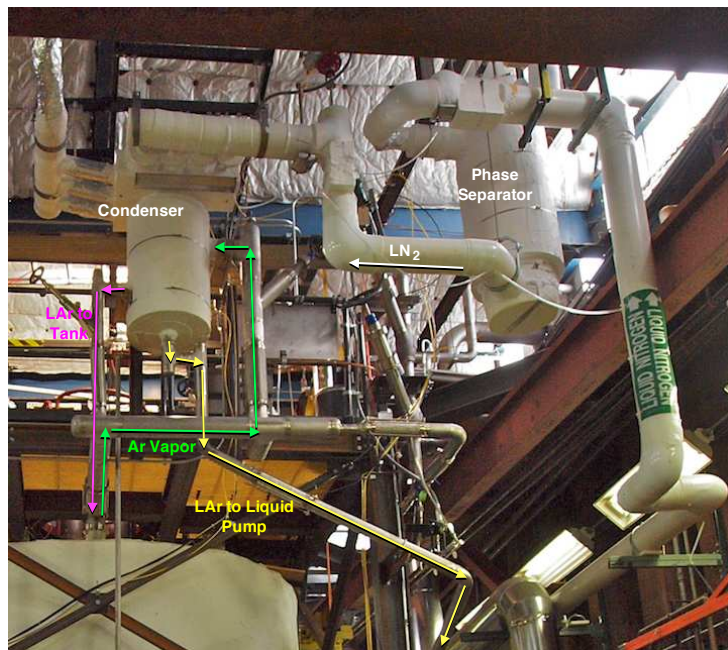


Figure 5. A photograph of the LAPD phase separator and condenser. The argon vapor path to the condenser and the two liquefied argon return paths are shown.

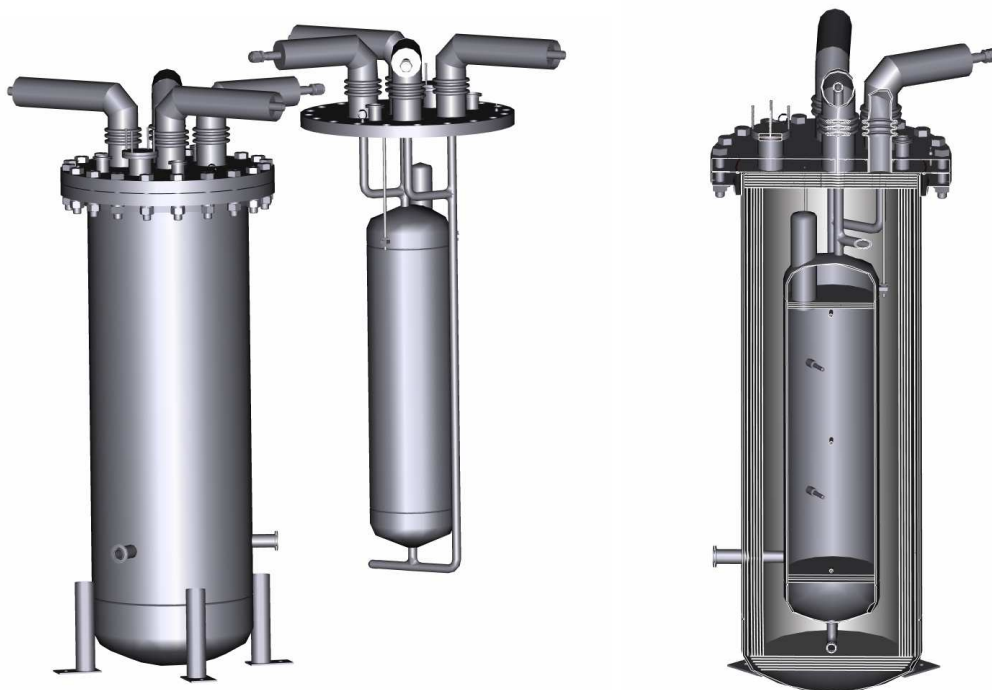


Figure 6. 3D model of the filter vessel. The evacuation vessel and the canister holding the filter material are shown on the left. The cross section of the vessel is shown on the right.

47 area. During the heated gas regeneration, five filter bed temperature sensors monitor the filter
1 material temperature and the water content of the regeneration exhaust gas is measured. Both
2 filters are evacuated using turbomolecular vacuum pumps while they cool to remove remaining
3 trace amounts of water.

4 At the filtered liquid return to the tank, a particulate filter with an effective filtration of
5 10 microns protects the tank from any debris in the piping. The filter consists of a commer-
6 cial stainless steel sintered metal cylinder mounted in a custom cryogenic housing and vacuum
7 jacket. Flanges on the argon piping along with flanges and edge welded bellows on the vacuum
8 jacket allow removal of the particulate filter. Liquid argon flows to the interior of the sintered
9 metal cylinder and then outward through the walls of the sintered metal cylinder which provide
10 filtration.

11 3.3. Piping and Valves

12 The Schedule 10 stainless steel purification piping that supplies argon to the filters is vacuum
13 jacketed. The inner line containing argon is 1 inch in diameter with a 3 inch diameter vacuum
14 jacket, except at the pump suction where the inner line is 2 inches in diameter with a 5 inch
15 diameter vacuum jacket. During the fabrication process, all piping was washed with deionized
16 water and detergent to remove oil and grease. Lint free rags wetted with alcohol were pulled
17 through the pipes until no contamination was visible on the rag. All valves associated with the
18 argon purification piping utilize a metal seal with respect to ambient air either through a bellows
19 or a diaphragm to prevent the diffusion of oxygen and water contamination. The exhaust side of
20 relief valves is continuously purged with argon gas such that diffusion of oxygen and water from
21 ambient air across the o-ring seal is prevented. Where possible, ConFlat flanges with copper
22 seals are used on both cryogenic and room temperature argon piping. Pipe flanges in the system
23 are sealed using spiral wound graphite gaskets (reference a part number). Smaller connections
24 are made with VCR fittings with stainless steel gaskets.

25 3.4. Recirculation Pump

26 The liquid argon pump is a Barber-Nichols BNCP-32B-000 long shaft argon pump. It is a
27 partial emission centrifugal pump with a magnetic drive to isolate the pump and liquid argon
28 from the electric motor. The pump shaft with the impeller, inducer and driven section of the
29 magnetic coupling have their own bearings which are lubricated by the liquid argon at the
30 impeller end and are non-lubricated at the coupling end. The motor is controlled by a variable
31 frequency drive (VFD) which allows adjustment of the pump speed to produce any desired head
32 and flow within the available power range of the motor. A photograph of the liquid pump is
33 shown as Figure 7.

34 The liquid argon flow rate is measured at the pump discharge by an Emerson Process Man-
35 agement Micro Motion Coriolis flow meter. This flow meter is appropriate for ultra high purity
36 liquid argon because, from the perspective of the liquid argon, it only consists of stainless steel
37 pipe and flanges. The inertial effects of the fluid flow through the flow meter pipes is directly
38 proportional to the mass flow of the liquid. The mass flow rate is computed by measuring the
39 difference in the phase vibration between one end of the flow pipe and the other. The flow
40 curve of the liquid argon pump with respect to mass flow and pressure is quite flat, such that
41 pump speed and differential pressure are not good indicators of the mass flow rate. Can we use
42 the manufacturer's plot with a proper reference? Thus the liquid argon flowmeter is essential
43 instrumentation if the rate of filtration is to be known.



Figure 7. A photograph of the recirculation pump housing.

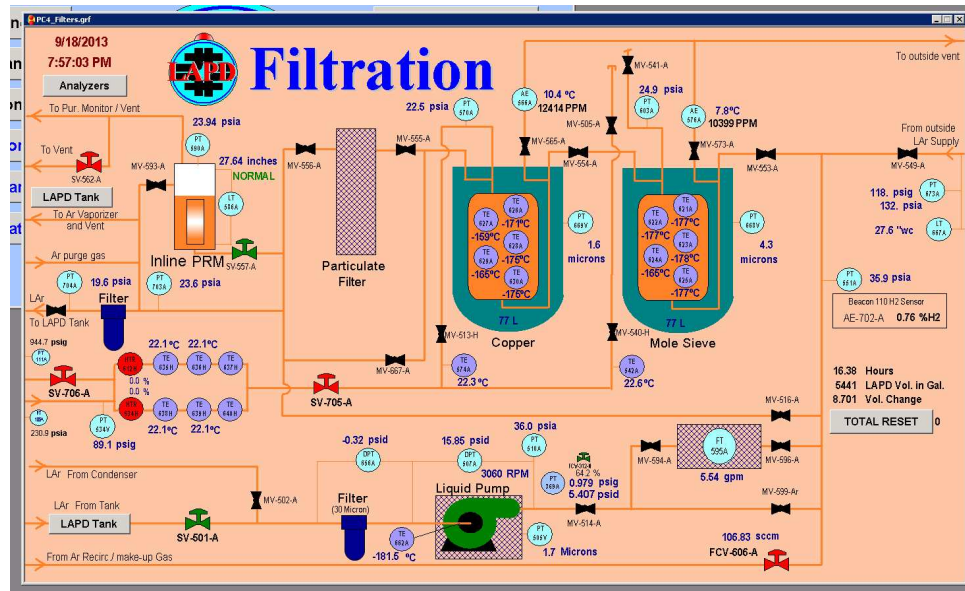


Figure 8. An example of iFIX graphical user interface for the LAPD controls.

3.5. Control System

The LAPD cryogenic system is controlled by a Siemens Programmable Logic Controller (PLC). The PLC reads out the pressure, liquid level, temperature, gas analyzer instrumentation, and electron lifetime measured by purity monitors. Human-machine interface controls are provided through GEFANUC's iFIX software running on a Windows PC, which is connected to the PLC through local ethernet. The iFIX software allows entry of temperature and pressure set points and other operational parameters, handles alarming and remote operator controls such as opening and closing valves, displays real-time instrument values, and archives instrument values for historical viewing. An example of the iFIX graphical user interface used in the LAPD is shown in Figure 8.

4. Cryostat Instrumentation

In this section we describe the instruments located inside the cryostat for the purity and temperature measurements including the purity monitors, the gas analyzers, and the resistive thermal device (RTD) translators. Figure 9 shows the locations of purity monitors and RTD translators inside the cryostat.

4.1. RTD Translators

This section needs to be shortened and wordsmithed. We installed two sets of three resistive thermal devices (RTDs) on translators which are deployed to measure thermal gradients in the cryostat at all stages of operation (gas purge, liquid filling, partially filled cryostat and full cryostat). When there is liquid in the cryostat, the RTDs measure the temperature of both the liquid and the gas in the ullage. One spooler is installed near the center of the cryostat and the other is installed 1.0 m radially outward from the center.

The motivation for installing these translators is to verify finite element analysis (FEA) calculations [11] used to model LAr mass flow in the cryostat. These calculations are important to

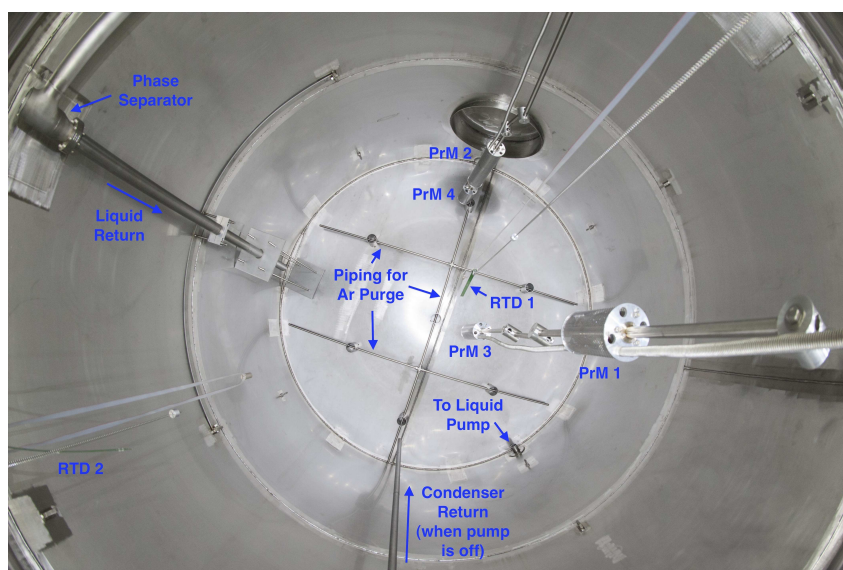


Figure 9. A photograph of the interior of the cryostat. The purity monitors, RTD translators and piping are shown.

24 understand if potential current eddies might occur under certain circumstances. These eddies
 1 might concentrate impurities or positive space charge in a TPC detector environment, leading to
 2 difficulty measuring ionization that passed through these regions. Gas flow in the ullage which
 3 can mix impurities into the liquid are also calculated by FEA [11]. **At this point, temperature
 4 gradients are the only experimental way to verify the calculations. LARTPC-doc-635-v4 has a
 5 prediction for temperature as a function of position. It may be good to overlay the prediction
 6 on Fig 12.**

7 Each translator consists of a single circuit board, 50 cm long with RTDs mounted at 22.9
 8 cm intervals for a total of 3 RTDs per circuit board as seen in Figure 10. The circuit board is
 9 suspended at one end of a chain, with a counter-weight at the other end of the chain to prevent
 10 movement during an electrical outage. The central chain is 3 m long and the radial chain is
 11 2.5 m long – the difference arises from the shape of the sloping top of the cryostat. The chains
 12 engage a 15.13 cm circumference gear that is driven externally, through a ferromagnetic seal,
 13 by an Automation Direct STP-MTRH-23079 stepper motor. The housing around the gear also
 14 includes electrical limit switches to stop the motor when the chain limits are reached. The
 15 stepper motor is controlled by an Automation Direct STP-DRV-4850 stepper drive. During a
 16 typical Spooler run, the circuit board translates vertically through the cryostat with stops at
 17 predefined locations to take temperature measurements.

18 A ribbon cable connects one end of the circuit board to a feed-through at the top of the
 19 cryostat, in the same stand as the stepper motor gear, and connects to a LakeShore model
 20 218 temperature monitor which reads out all six RTDs. The stepper motor controller and
 21 LakeShore are controlled and read out by a custom LabVIEW application (“Application”). The
 22 Application has a graphical interface to display both the temperature measurements and motor
 23 drive conditions and writes data files which are then accessible by network for offline analysis.

24 The RTDs are platinum, type K 100 Ohm and were not calibrated, either from the manu-
 25 facturer or by us before their use. However, the RTD devices were immersed in liquid nitrogen



Figure 10. A photograph of the peripheral RTD translator inside the LAPD cryostat.

26 upon their arrival and found to be accurate to within 0.5 Kelvin. For the data presented here,
1 the temperature offsets at LAr temperatures were adjusted in software to overlap for all three
2 RTDs on a single Spooler. It should be noted that the LAr in the LAPD cryostat is not at
3 thermal equilibrium since the vapor is continually being removed and condensed in an external
4 condenser, then admixed with LAr drawn directly from the cryostat and then sent through pu-
5 rification filters before being returned to the cryostat. This evaporation of LAr from the surface
6 is seen visually by a surface turbulence, and detected by the Spooler RTDs as a temperature
7 drop both from the bulk liquid below the surface, and the vapor above in the ullage.

8 The RTD circuit board is normally parked at the top limit switch. During a typical run,
9 the Application moves the RTD circuit board twenty equal steps downward, and then reverses
10 direction and moves the Spooler up using the same number and size of the steps. At each step
11 motion, the Application pauses for a predetermined wait-after-move time. After this pause, the
12 three RTDs of a single Spooler are scanned sequentially. In order to improve the precision of
13 the temperature measurement, the Lakeshore was setup to average (in an exponential window)
14 up to 64 points per RTD readout. After this scan, the application waits another period of time.
15 This wait time was chosen to be long enough to ensure the exponential averaging window has
16 been filled with new data points. Then the three RTDs are scanned again. This is repeated one
17 more time so that at any vertical position, each RTD is measured three times.

18 The motivation for the three measurements of each RTD at every vertical location is that it
19 is useful to see if the temperature is constant over this period, both to understand the inherent
20 precision of the measurement, but also to see that the RTDs are in actual thermal equilibrium
21 with the argon. In the case of determining the measurement precision, one expects a random
22 scatter of temperature versus the measurement order, while in the case of non-thermal equilib-
23 rium, the variation of RTD temperature versus the measurement order monotonically increases
24 or decreases. In the case that the RTD is in the liquid, the RTD appears to quickly come to
25 thermal equilibrium even for relatively short wait periods, since the thermal heat transfer with
26 liquid is very good. However in the gas, the thermal heat transfer is much slower. This is
27 exacerbated by the circuit board material that the RTD is in close proximity with. In order
28 to make precise measurements in the gas, the wait-after-move time needed to be 30 minutes,
29 particularly where the temperature gradient was high. In general the wait-after-move time was
30 setup to be much less than this, since our main concern was with any temperature gradient in
31 the liquid. Waiting long periods of time introduces other issues with variations of the cryostat
32 total internal pressure (barometric and internal gauge pressure). At the level of 5-10mK, these
33 variations impact the temperature. Due to thermal lags, it is difficult to accurately correct for
34 pressure variations even though we knew the total pressure during the time of the run.

35 Figure 11 shows a scan of the cryostat taken after the first fill of LAr level for the cen-
36 tral and peripheral RTD translators. Of primary note is the very sharp temperature gradient
37 (80K/50cm) in the ullage just above the liquid surface. The top of the LAr surface was 2.9m
38 (115") below this point at the date of this particular run. The data shown were taken only
39 from the downward direction of the total run, to avoid the thermal lag one sees when the circuit
40 board is moving out of the liquid. The wait-after-move time was 5 minutes in this case.

41 Figure 12 shows a relatively quick scan with the cryostat full and the wait-after-move time
42 of 3 minutes. It should be noted that the lowest RTD of this Spooler is located just slightly
43 above the LAr level, even with the circuit board at the top of the limit switch. However the
44 lower tip of the circuit board is just dipping or very near the liquid surface. As a result of
45 the heat conduction in the circuit board, this lower RTD temperature is biased lower than it
46 would actually be if the circuit board tip were not there. As the circuit board is lowered into
47 the LAr, one can see the temperature dip 0.4K below the temperature of the bulk liquid. This

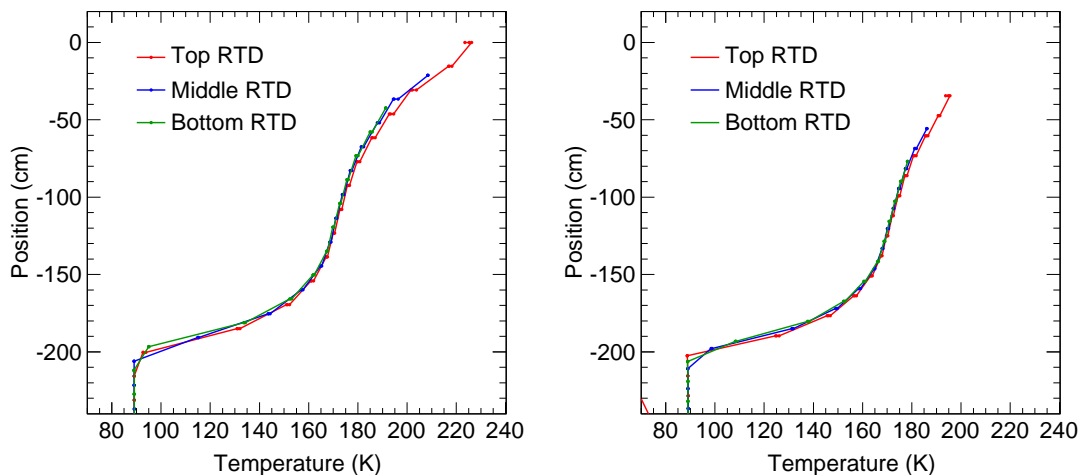


Figure 11. The cryostat temperature as measured by the three central (left) and the three peripheral (right) RTDs. **Need to specify fill level of LAr. Also put lines on plots indicating the liquid level.**

48 is just the evaporative cooling of the surface layer of the LAr. Once the RTDs penetrate this
 1 surface layer, the temperature recovers to almost a constant value. It temperature scale should
 2 be noted here. The slight change of temperature with depth is less than approximately 25mK
 3 over 2m. At the bottom of the scan there is another dip of 30mK. The returning purified LAr
 4 is introduced at the bottom of the cryostat and may be the cause of this slight dip. Looking
 5 at the spread in measurements of any one RTD at a fixed position in the liquid, the peak-to-
 6 peak spread is 10mK, implying the relative precision of a single measurement is on the order
 7 of a few mK. There is a nominal agreement between our measurements and FEA calculations
 8 ([?]). This gives confidence that we can use the FEA with some confidence in actual detector
 9 configurations.

10 4.2. Purity Monitors

11 4.2.1. Hardware

12 A dedicated monitoring device, called a purity monitor, is used to determine the purity of the
 13 LAr. The purity monitor is a double-gridded ion chamber immersed in the liquid argon volume
 14 based on the design described in Reference [9]. It consists of four parallel, circular electrodes:
 15 a disk supporting a photocathode, two open wire grids (anode grid and cathode grid) and an
 16 anode disk. The anode disk and photocathode support disk are made of stainless steel; the two
 17 grid support rings are made of G-10 circuit board material with the grid wires soldered to the
 18 copper clad surface. The region in between the anode grid and cathode grid contains a series
 19 of field-shaping stainless steel rings. The two grids, each with a single set of parallel wires, are
 20 made of electro-formed gold-sheathed tungsten (AuW) with a 2.0 mm wire spacing, 25 μm wire
 21 diameter and 98.8% geometrical transparency (see Table 1).

22 The cathode grid is at ground potential. The cathode, anode grid, and anode are electrically
 23 accessible via modified vacuum grade high voltage feed-throughs. The anode grid and the field-
 24 shaping rings are connected to the cathode grid by an internal chain of 50 M Ω resistors to ensure

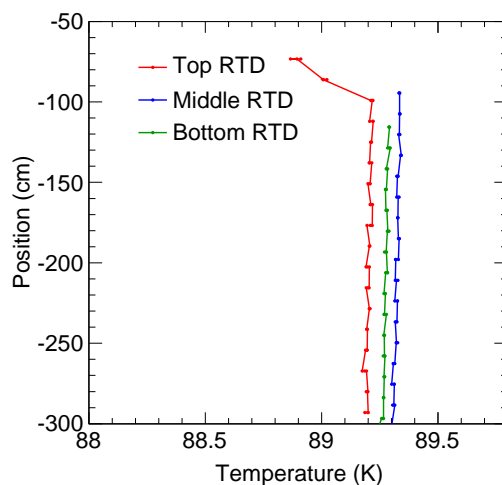


Figure 12. The temperature as measured by the three central RTDs when submerged in liquid argon. This figure illustrates the precision with which the temperature is measured. **What are the points at the top?**

25 the uniformity of the electric fields in the drift regions. The field ratios typically satisfy

$$1 \quad E_{Anode \text{ Grid}-Anode} > 2E_{Anode \text{ Grid}-Cathode \text{ Grid}} > 4E_{Cathode \text{ Grid}-Cathode} \quad (1)$$

2 to ensure maximum transparency [10].

3 **footnotes will become endnotes** The photocathode³ is a 1" × 3" × 1/32" aluminum slide,
 4 coated with 50 Å of titanium and 1000 Å of gold and attached to the cathode disk. A xenon
 5 flash lamp⁴ is used as the light source. The UV output of the lamp has a wide spectrum above
 6 approximately 225 nm. An inductive pickup coil on the power leads of the lamp provides a
 7 trigger signal when the lamp flashes. Light is directed via three quartz optical fibers⁵ to the
 8 photocathode. Only one fiber is needed the other two are for redundancy. The fibers have a 0.6
 9 mm core diameter and 25.4 degrees of full acceptance cone. The attenuation is 0.95 dB/m at λ
 10 = 200 nm. The electrons liberated from the photocathode drift towards the cathode grid and
 11 induce a current on the cathode. After crossing the cathode grid, the electrons drift between
 12 the two grids. During this time essentially no current is induced on the cathode or anode due
 13 to the shielding effect of the grids. After crossing the anode grid, the electrons induce a current
 14 on the anode. The signals induced on the cathode and anode are fed into two charge amplifiers
 15 in a purity monitor electronics module. The charge amplifiers have a 5 pF integration capacitor
 16 with a 22 M Ω resistor in parallel with the capacitor. The signal and high voltage are carried on
 17 the same cable and decoupled inside the purity monitor electronics module. Figure 13 shows a
 18 schematic of the liquid argon purity monitor.

19 The LAPD system employs five purity monitor units at different locations. Each purity
 20 monitor is contained in a stainless steel, perforated Faraday cage to isolate the system from the
 21 outside electrostatic interference. There are two types of purity monitors with different lengths

³Made by Platypus Technologies, LLC, Madison, WI

⁴Made by Newport, Stratford, CT

⁵Made by Polymicro Technologies, Phoenix, AZ

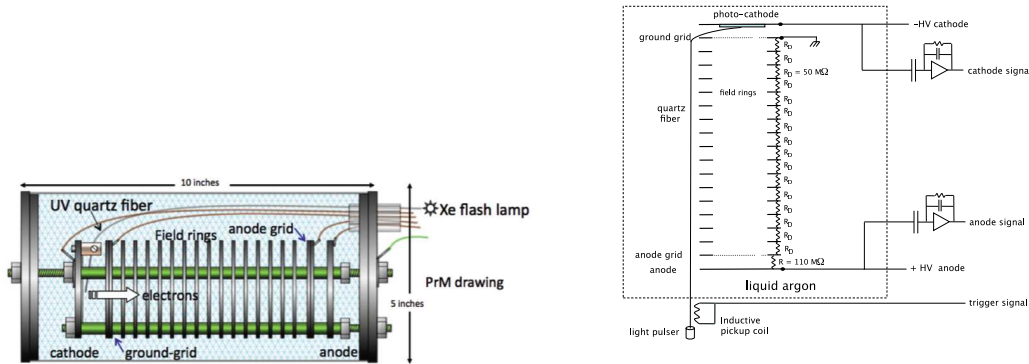


Figure 13. Drawing and schematic of Liquid Argon Purity Monitor.

22 and different numbers of field-shaping rings: three long purity monitors that are 55 cm and two
 1 short purity monitors that are 24 cm. **T/F? necessary? The longer electron drift time in the**
 2 **long purity monitor ensures a more accurate lifetime measurement.** An assembly of one long
 3 purity monitor and one short purity monitor is located vertically along the central axis of the
 4 cryostat. Another identical assembly is located at a distance of 1.1 m away from the center of
 5 the cryostat. Figure 14 shows a photograph of the assembly located near the cryostat periphery.
 6 One long purity monitor, referred to as the inline purity monitor, is located in the circulation
 7 pipe to measure the liquid Argon purity before the liquid enters the cryostat. Three flash lamps
 8 are used for the two purity monitor assemblies and the inline purity monitor. Table 1 shows the
 9 geometrical characteristics and voltage settings of the purity monitors installed in the cryostat.

10 4.2.2. Data Acquisition

11 A Visual Basic program running on a Tektronix⁶ digital storage oscilloscope (5054 TDS) is
 12 used for control and data acquisition for the purity monitor system. The program controls
 13 operations through the Fermilab-designed automation module, which controls the high voltage
 14 power to the purity monitor and the flash lamp operation. Measurements of the electron lifetime
 15 are taken several times a day. Each measurement of the lifetime takes about one minute. The
 16 flash lamp and the high voltage to the purity monitors are only powered during this time
 17 to protect the flash lamp, minimize degradation of the quartz fiber and reduce dust/particle
 18 accumulation on the purity monitor. **why?** The automation module will switch off both the flash
 19 lamp power supply and high voltage to the purity monitor if the lamp has been flashing for more
 20 than 140 seconds.

21 An 8-channel analog MUX **define this** is used to select which purity monitor signal is readout.
 22 Each channel of the MUX has four inputs, three of which read the cathode and anode signals
 23 from one purity monitor after the amplifiers and the trigger signal from the inductive pickup
 24 coil. The program communicates with the MUX through the 5054 parallel port and sends a
 25 signal to the MUX to select one of the five purity monitors. The MUX then sends a signal to
 26 the automation module to switch on the high voltage power to the selected purity monitor and
 27 flash lamp. The MUX also sends the relevant trigger, cathode, and anode signals to the scope.

⁶Tektronix, Inc., Beaverton, OR



Figure 14. One assembly of one long purity monitor and one short purity monitor inside LAPD.

Table 1
Geometrical characteristics and voltage settings of the purity monitor.

	Long monitor	Short monitor
Cathode, Anode disk, grid diameter		8 cm
Cathode-Anode total drift distance	50 cm	19 cm
Cathode grid to Anode grid distance	47 cm	16 cm
Cathode-Cathode Grid gap		1.8 cm
Anode Grid-Anode gap		0.79 cm
Number of field-shaping rings	45	15
Number of resistors	46	16
Anode disk/Cathode disk thickness		0.23 cm
Anode grid/Cathode grid thickness		0.24 cm
Field-shaping ring thickness		0.23 cm
Gap between rings		0.79 cm
Nominal Cathode Voltage	-100 V	-100 V
Nominal Anode Voltage	5 kV	2 kV
$V_{Anode\ Grid}/V_{Anode}$	0.948	0.865
Nominal $E_{Cathode\ Grid-Cathode}$	56 V/cm	56 V/cm
Nominal $E_{Cathode\ Grid-Anode\ Grid}$	101 V/cm	108 V/cm
Nominal $E_{Anode\ Grid-Anode}$	329 V/cm	342 V/cm

28 The program in the TDS 5054 oscilloscope digitizes the signals after the high voltages sta-
 1 bilize and calculates the electron lifetime (τ) based on the ratio of anode and cathode signals
 2 ($Q_{anode}/Q_{cathode}$) and the electron drift time (t), the time between the cathode and anode sig-
 3 nals, using the relation [9]

$$4 \quad Q_{anode}/Q_{cathode} = e^{-t/\tau}. \quad (2)$$

5 The program turns on each purity monitor and reads out the signals one by one. Figure 15
 6 shows the block diagram of LAPD purity monitor system.

7 During the initial operation, we observed the presence of large noise components generated by
 8 the flash lamp particularly in the cathode and anode signals. The noise affects the waveforms
 9 and makes it difficult to measure the amplitudes of the signals. We modified the automation
 10 module and the DAQ program to measure the noise before measuring the signals. The program
 11 first sends out a signal to the MUX to ask the automation module to switch on the flash lamp
 12 power supply without switching on the high voltage power to the purity monitor. The scope
 13 stores the waveforms, which provide an estimate of the noise. Then the program sends out
 14 another signal to turn on the high voltage power to the purity monitor in addition to the flash
 15 lamp. The noise is then subtracted from the measured waveforms to get the real cathode and
 16 anode signals.

17 For the **second run, which needs definition** of LAPD, the purity monitor DAQ system, previ-
 18 ously consisting of a Tektronix oscilloscope, was replaced by a PC equipped with a PCI digitizer
 19 card. The digitizer card is a 12-bit AlazarTech ATS310 card capable of sampling at 20 MHz.
 20 The new DAQ system performed as well as the oscilloscope and was procured at a cheaper cost.
 21 The original Visual Basic purity monitor DAQ program from the first run was modified to run
 22 with the digitizer utilizing the development kit for the ATS310.

23 For each acquisition, the digitizer recorded and averaged at least ten samples for each of the

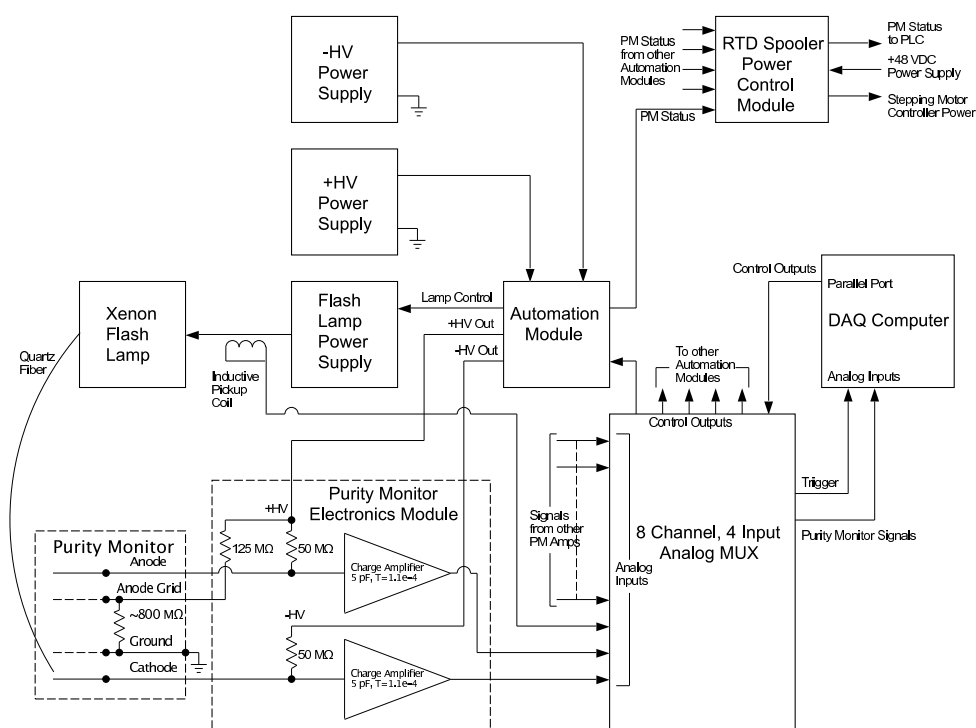


Figure 15. Block diagram of LAPD purity monitor system.

24 traces needed. For the long purity monitors, the sampling rate used was 2 MHz and for the
 1 short purity monitors, 5 MHz. The range of voltages used used for both long and short purity
 2 monitors was ± 50 mV. A plot of the averaged signal traces produced from the digitizer card,
 3 before and after noise subtraction, is shown in Figure 16.

4 An additional source of electrical noise that affected the operation of the purity monitor DAQ
 5 was found to be the RTD spooler stepper motor controllers. These controllers have a DC to
 6 DC switching converter that provides the holding current to the stepper motors used in the
 7 RTD spooler system. The most effective way to mitigate this noise source was to remove the 48
 8 volt DC bulk power to the stepping motor controllers whenever the purity monitor DAQ was
 9 running. After the purity monitors were turned off by the DAQ, the 48 volt DC power was
 10 restored to the stepping motor controllers and a reset signal was given to the controllers so that
 11 they would reindex back to the zero starting point for their data collection.

12 4.2.3. Fiber Quality checks

13 We use three single-mode quartz optical fibers to illuminate the each purity monitor photo-
 14 cathode. The fibers underwent a series of tests to measure the stability and light output linearity
 15 as a function of input light intensity. The tests were performed using a simple analog photodiode
 16 read out by an oscilloscope. Fibers were positioned with one end in close proximity to the light
 17 source and the other end in close proximity to the photodiode. Measurements of the photodiode
 18 response for a single fiber were taken for several values of relative input intensity as reported
 19 on the mercury lamp light source with results suggesting a linear response. The variation in the
 20 photodiode response was measured by recording ten consecutive measurements for each fiber

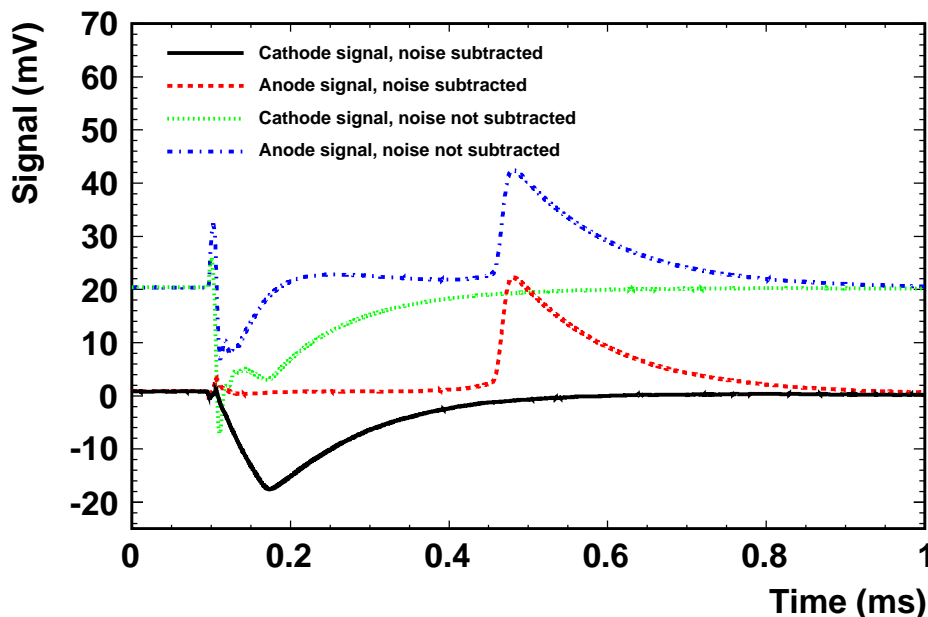


Figure 16. A screenshot of anode and cathode signals before and after noise removal from the digitizer. **The third legend entry is hard to see.**

21 and showed maximum relative deviations of 5%. Finally, for each fiber, the photodiode response
 1 was measured with the light source placed in a vertical configuration and a horizontal config-
 2 uration and showed no changes. The fiber cleaves were inspected and showed no anomalous
 3 behavior. However, three fibers indicating a nominal response had a small, sharp edge sticking
 4 out. The fiber with the highest response had the opposite, much like a small “chip” out of the
 5 edge. These studies suggest that the employed fibers were suitable for accurately delivering the
 6 light from the lamp to the photocathode. **There are plots of each of these studies that I chose**
 7 **not to include.**

8 4.2.4. Systematic Uncertainties

9 There are several systematic effects which need to be accounted for to make a reliable mea-
 10 surement of argon purity. The lifetime relies on measurements of V_{anode} and $V_{cathode}$, which in
 11 turn depend on amplification of induced currents on the anode and cathode. The potential exists
 12 for differences in amplification between the anode and cathode signal voltages to have an impact
 13 on the lifetime. We model the amplification as $V_{anode} = g^\alpha Q_{anode}$ and $V_{cathode} = g^\beta Q_{cathode}$,
 14 where g^α and g^β are constants. If the two amplifiers used for the anode and cathode signals are
 15 switched, the amplification becomes $V'_{anode} = g^\beta Q_{anode}$ and $V'_{cathode} = g^\alpha Q_{cathode}$. The primes
 16 indicate measurements taken with the amplifiers for the anode and cathode swapped.

17 The lifetime and attenuation calculations can then be calibrated by making measurements of
 18 V_{anode} , V'_{anode} , $V_{cathode}$, and $V'_{cathode}$ using

$$19 \frac{g^\alpha}{g^\beta} = \sqrt{\frac{V_{anode}/V_{cathode}}{V'_{anode}/V'_{cathode}}}. \quad (3)$$

20 During a span of several days at nearly constant argon purity, measurements were taken with
 1 the amplifiers swapped to measure the ratio g^α/g^β . With the measurements taken, a correction
 2 to the lifetimes was applied using

$$3 \quad \tau = \frac{t}{\ln((V_{cathode}/V_{anode}) \times (g^\alpha/g^\beta))}. \quad (4)$$

4 Another systematic uncertainty examined is the effect of the values of the high voltages applied
 5 to the cathode and anode. To examine this effect, the high voltages applied to the anode and
 6 cathode were varied and many measurements were taken during a span of a few hours with
 7 relative constant purity. A short purity monitor was run with high voltages on the anode at
 8 2 kV, 3 kV, 4 kV, and 5 kV. **We need a conclusion with some percentages along with the 1.028**
 9 **correction.**

10 4.3. Gas Analyzers

11 4.3.1. Oxygen, Water and Nitrogen Monitors

12 LAPD has an extensive gas analysis system to monitor and diagnose the processes that take
 13 the cryostat from atmospheric air to ultra pure liquid argon. The system consists of seven com-
 14 mercial gas analyzers. Four of these analyzers measure the oxygen concentration and together
 15 they span the range from 0.1 ppb to 5000 ppm. These four oxygen analyzers are augmented by
 16 two 0.1-25% oxygen sensors which monitor the purge of the cryostat of air and are described in
 17 Sec. 4.3.2. Two of these seven gas analyzers measure the water concentration and these span the
 18 range from 0.2 ppb to 20 ppm. Dew point meters installed in series with these water analyzers
 19 extend the measurement range from 20 ppm up to ambient dew points as high as 20,000 ppm
 20 water. A nitrogen analyzer completes the array of seven gas analyzers with a range that spans
 21 0.1 to 100 ppm.

22 The gas analyzers are fed by a local switchyard of 56 diaphragm valves. These valves direct
 23 the gas flow from five primary locations in the system to the seven gas analyzers. In addition to
 24 the five primary locations, argon and nitrogen gas from utility sources are available to supply
 25 analyzers when measurement from a system location is not required. A primary location or util-
 26 ity gas can feed anywhere between none and all of the gas analyzers. The primary measurement
 27 locations are the liquid argon cryostat, with the option of sampling from either the gas or liquid
 28 phases, pump discharge, molecular sieve filter output, oxygen filter output, and the liquid argon
 29 fill connection. An oil free vacuum pump is also part of the switchyard and can evacuate the
 30 tubing that connects the measurement locations and the gas analyzers. Evacuation of the sam-
 31 ple lines when switching sample locations greatly reduces the time required to reach equilibrium
 32 when the measured contamination is at the parts per billion concentration. A high purity metal
 33 bellows pump boosts the sample pressure from the 2 psig operating pressure of the liquid argon
 34 cryostat to the 15-20 psig inlet pressure required by the gas analyzers. A photograph of the gas
 35 distribution switchyard is shown in Figure 17.

36 Filter output sampling allows determination of filter performance and capacity. Sampling the
 37 liquid argon fill connection is critical to ensure that the liquid argon supply is within specification.
 38 For example, a trailer of liquid argon was rejected because it was so far out of specification it
 39 would have required an impractical number of filter regenerations to process. Without this
 40 extensive gas analyzer system it would be very difficult to successfully take the cryostat from
 41 ambient air to ultra pure liquid argon.

42 4.3.2. Oxygen Capillary Detectors

43 We deployed 14 industrial type (Citicell model 2FO) oxygen sensors, configured in two strings
 44 of 7 each consisting of capillary tubes placed at different heights, to measure the oxygen concen-

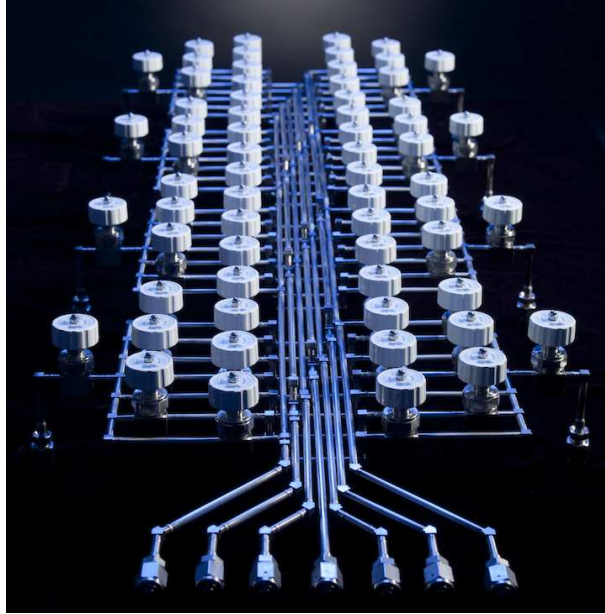


Figure 17. Gas distribution switchyard - liquid argon gas sampling master distribution panel.

45 tration during the initial gaseous argon purge. One string was placed near the cryostat wall and
 1 the other was placed near the cryostat center. Their vertical spacing is about 30 inches spanning
 2 the height of the cryostat. The central set was placed on the tank axis, the peripheral set was 44
 3 inches radially out. The sampling tube inlets were spaced 30 inches apart, spanning the height
 4 of the tank. The sensors are inside glass “jam jars” with plastic coated lids. The sample tubes
 5 are 0.063 inch diameter capillaries, and run continuously from the intake point through a CF
 6 flange to the jars. All capillaries are the same length, with the excess length coiled up above the
 7 feed-through flange, to assure matched time response. The jars are mounted on feed-through
 8 flanges.

9 5. Results from Operation Modes

10 The LAPD was operated in two separate run periods. In each period, the cryostat was oper-
 11 ated in three phases; a gaseous argon purge, gaseous argon recirculation, and liquid recirculation.
 12 The first run period was September 2011 to April 2012. Each of the three phases of operation
 13 were performed to test the devices and filters. For this period, the cryostat was filled 1/3 full
 14 to confirm the feasibility of measuring the liquid argon purity **Need a little more motivation**
 15 **and explanation of relevant events here**. The second period was from December 2012 through
 16 October 2013. For each period, we performed a single argon purge at the beginning of the pe-
 17 riod, followed by a single phase of gaseous argon recirculation. The cryostat was then filled with
 18 liquid argon and measurements of the liquid argon purity were performed under various operat-
 19 ing conditions. This section describes the results for the second period, and when applicable,
 20 measurements are compared to those obtained in the first run period.

21 **5.1. Gaseous Argon Purge**

1 A gaseous argon purge was performed at the beginning of each run period. In this phase of
 2 operation, gaseous argon is pumped from the bottom of the cryostat displacing the ambient air
 3 which exits out the room temperature feedthroughs at the top of the cryostat. This method
 4 mimicks an argon “piston” in the sense that the higher density gaseous argon engenders a
 5 boundary between it and the ambient air, which moves vertically upwards. For the first time
 6 interval, the two sets of sampling gas capillaries described in section 4.x.x were installed to
 7 measure the oxygen concentration and follow the rise of the argon gas as it displaces the lighter
 8 room air.

9 The purpose of these measurements was to understand the average gas purity and obtain
 10 information for comparison to FEA flow models to validate or improve those models. The spatial
 11 and temporal concentration measurements provide information about the degree of diffusion
 12 and mixing during purges. Each purge lasted approximately 8 volume exchanges (~24 hours)
 13 and corresponds to a 3.8 ft/hour piston rise rate and 2.9 (3.4) hours per volume exchange for
 14 the first (second) run period. The gaseous argon flow rate was constant throughout each purge.
 15 Figure 18 shows the fraction of ambient air retained with respect to the measured oxygen levels
 16 during the gaseous argon purge in the first run period for the seven capillary tubes installed in
 17 the central region of the cryostat and the six, explain capillary tubes installed in the peripheral
 18 region of the cryostat. Insert a couple of tables for the positions? The front of gaseous argon
 19 is clearly present as indicated by the successive reduction of air seen by each capillary tube as a
 20 function of time. After 2.75 volume exchanges, corresponding to 8 hours, the oxygen level was
 21 reduced from 21% to xx ppm.

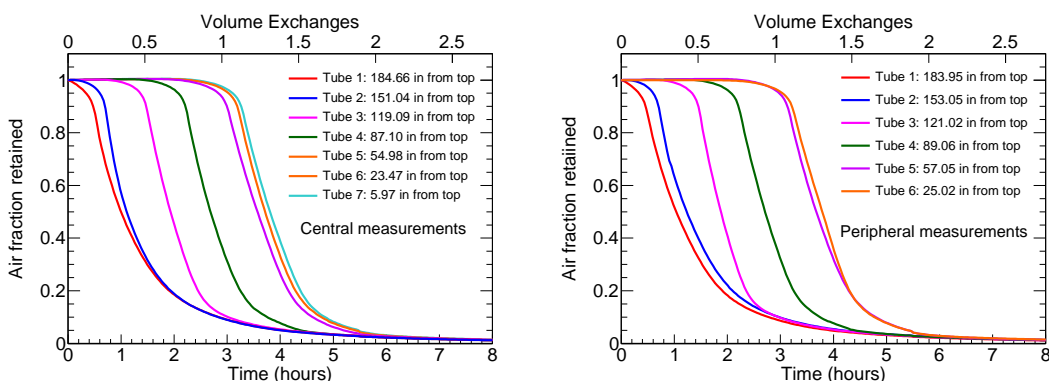


Figure 18. Oxygen concentrations for the a) central and b) peripheral gas sampling capillaries taken at several heights with respect to the cryostat bottom obtained during the initial gaseous argon purge for the first run period.

22 At the end of the purge, the capillaries were removed. This procedure lasted 15 minutes,
 23 during which time argon gas flowed into the cryostat at 5-6 SCFM. During the extraction, the
 24 water, oxygen, and nitrogen monitors were switched to argon gas utility as a precaution because
 25 the bellows pump drawing gas from the cryostat could pull a vacuum on the cryostat if the
 26 argon flow into the cryostat stopped. After these devices were switched back to measuring

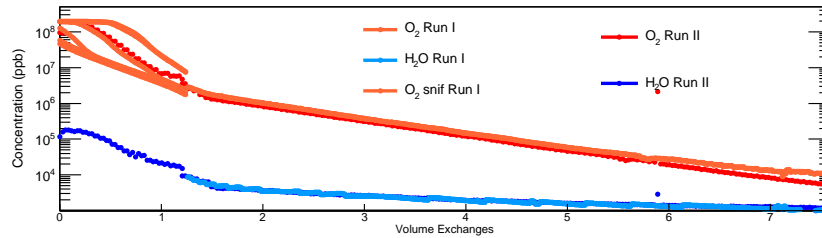


Figure 19. Water and oxygen concentrations in the LAPD during the two gaseous argon purges. Probably does not look good in black and white. Also two noise points?

27 the cryostat gas, an increase of about 0.2 ppm O₂ and 0.4 ppm N₂ was observed. With the
 1 capillaries removed, the makeup gas flow dropped from 0.35 SCFM to 0.15 SCFM. At the end
 2 of the purge, 7158 ft³ had passed through the cryostat, corresponding to 8.2 volume exchanges.
 3 The oxygen level was reduced to 5.2 ppm, the water concentration was reduced to 996 ppb,
 4 and the nitrogen concentration was reduced to 13.4 ppm. Figure 19 shows the concentrations
 5 of water and oxygen during the two gaseous argon purges along with the results from the
 6 capillary tube oxygen measurements. In both run periods the water concentration was reduced
 7 to approximately 1 ppm. The oxygen concentrations were reduced to 10(7) ppm for the first
 8 (second) run period. Throughout both purges, the nitrogen concentration remained nominally
 9 stable at 18 ppm. The argon purges for both run periods delivered similar results.

10 5.2. Gas Recirculation

11 After the removal of the ambient air from the argon purge, argon gas was pumped through
 12 the molecular sieve and oxygen filter at a rate of a volume exchange every 3.4 hours, then
 13 returned to the cryostat. The gas recirculation for the second run period ran for about 77
 14 volume exchanges or one week. Figure 20 shows the oxygen and water concentrations, measured
 15 by the HaloTrace and Nanotrace, for the gas recirculation phase. At the end of this phase,
 16 the oxygen concentration was reduced to approximately 20 ppb. The water concentration was
 17 stable at 667 ppb. This result indicates that water outgasses from all surfaces of the cryostat and
 18 piping. Note also that the outgassing rate eventually matches the filtration rate. The nitrogen
 19 was reduced to 13.7 ppm.

20 Figure 21 shows the water and oxygen concentrations measured in the gas in the cryostat
 21 vapor space. Need to describe these plots, in terms of the switching the devices from measuring
 22 in the liquid to measuring in the gas. This is for events in February and March

23 Figure 22 shows the water and oxygen concentrations measured in the gas in the cryostat
 24 vapor space. Need to describe these plots, in terms of the switching the devices from measuring
 25 in the liquid to measuring in the gas. This is for events in August and September.

26 5.3. Liquid Argon Filling

27 Need to describe filter loading calculations, the pump speed tests, and the result that speed
 28 doesn't affect purity

29 For the first run period, the cryostat was only filled to 1/3 capacity, which ended untimely
 30 due to a power outage. For the second run period, the cryostat was filled with LAr from the D0
 31 calorimeter at Fermilab. The duration of each fill varied from 4 to 6 hours. Table 2 presents the
 32 LAr trailer contaminant concentrations along with details of each successive fill for the second

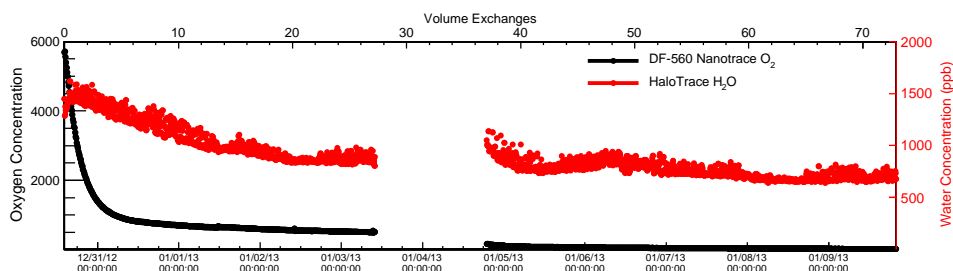


Figure 20. The water and oxygen concentrations in the cryostat gas during the gas recirculation phase of Run Period 2. Should be log scale? Also need explanation for the gap.

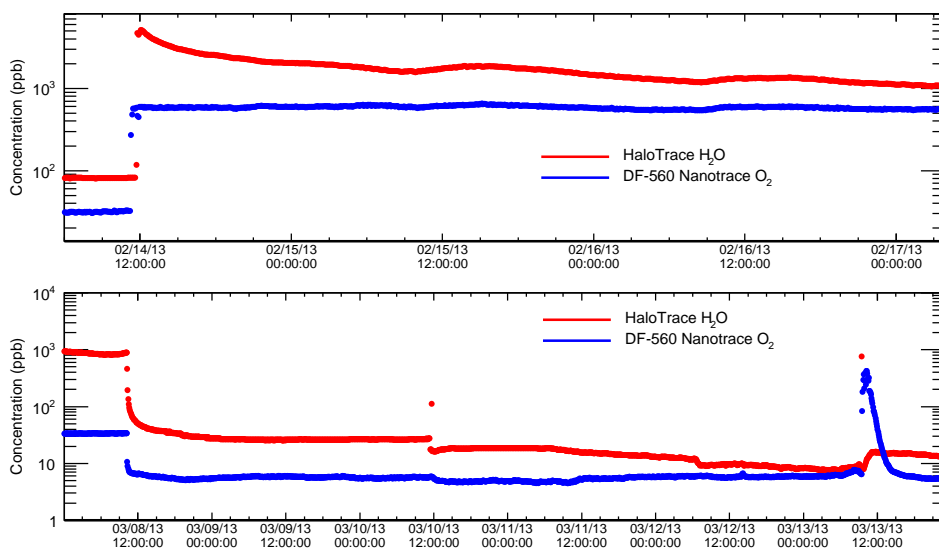


Figure 21. The water and oxygen concentrations in the gas of the vapor space at the top of the cryostat with the cryostat **totally filled**. Measurements were taken in the cryostat vapor at the 29 inch feed through and then on February 14, 2013 in the cryostat vapor at the top of the TPC feed through.

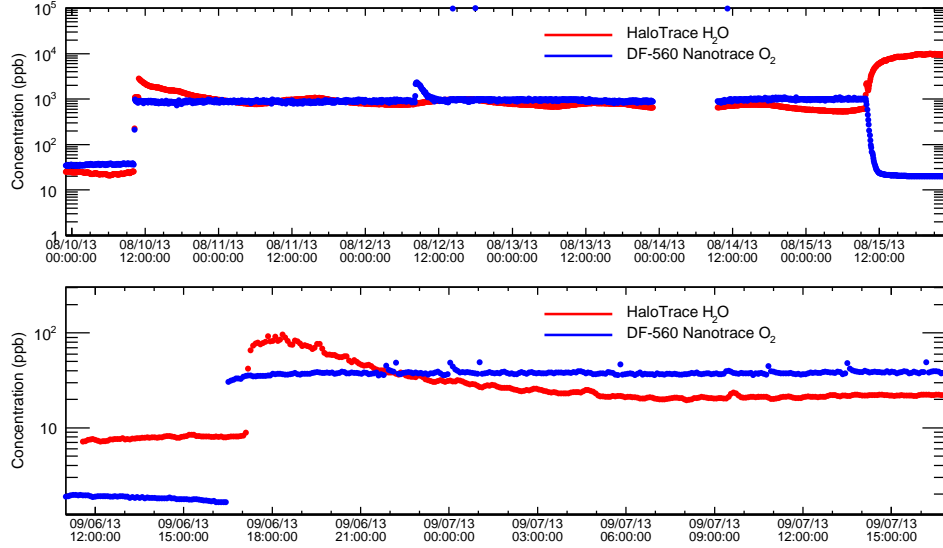


Figure 22. The water and oxygen concentrations in the gas of the vapor space at the top of the cryostat with the cryostat **totally filled**.

33 run period. The four trailers were delivered over a period of two weeks in January, 2013. The
 1 total volume of LAr placed in the cryostat was 5630 gallons, corresponding to 29.7 tons.

2 5.4. Liquid Argon Recirculation

3 After the cryostat was full, the liquid recirculation pump was started at a rate of 9.4 GPM.
 4 Filtration proceeded by routing liquid argon through the **two filters**. We had several opportuni-
 5 ties to determine the performance of the filters and their capability to reduce the impurities, at
 6 various times throughout operation. Figure 23 shows the water and oxygen concentrations in
 7 the cryostat liquid as measured by the **HaloTrace and Nanotracer** as a function of time, for three
 8 select intervals immediately preceding purity monitor operation. The measured oxygen concen-
 9 tration was compared to simulation assuming perfect mixing in the cryostat (**Need explanation**
 10 **for “perfect mixing”**). The figure shows that in the first two time intervals, perfect mixing was

	O_2 (ppb)	H_2O (ppb)	N_2 (ppm)	LAr height (inches)	GPF	Rate (GPM)	Net gallons
Trailer 1	202	99	10	27	1325	≈ 500	1325
Trailer 2	200	225	9	58	2832	587	1507
Trailer 3	400	180	9	87	4259	520	1427
Trailer 4	197	66	10	115	5630	400-525	1371

Table 2

Concentrations of oxygen, water, and nitrogen measured in each trailer before introduction into LAPD. The LAr height is measured in inches from the bottom of the cryostat corresponding to the number of gallons delivered to the cryostat in each fill (GPF). Also shown is the rate in gallons per minute (GPM).

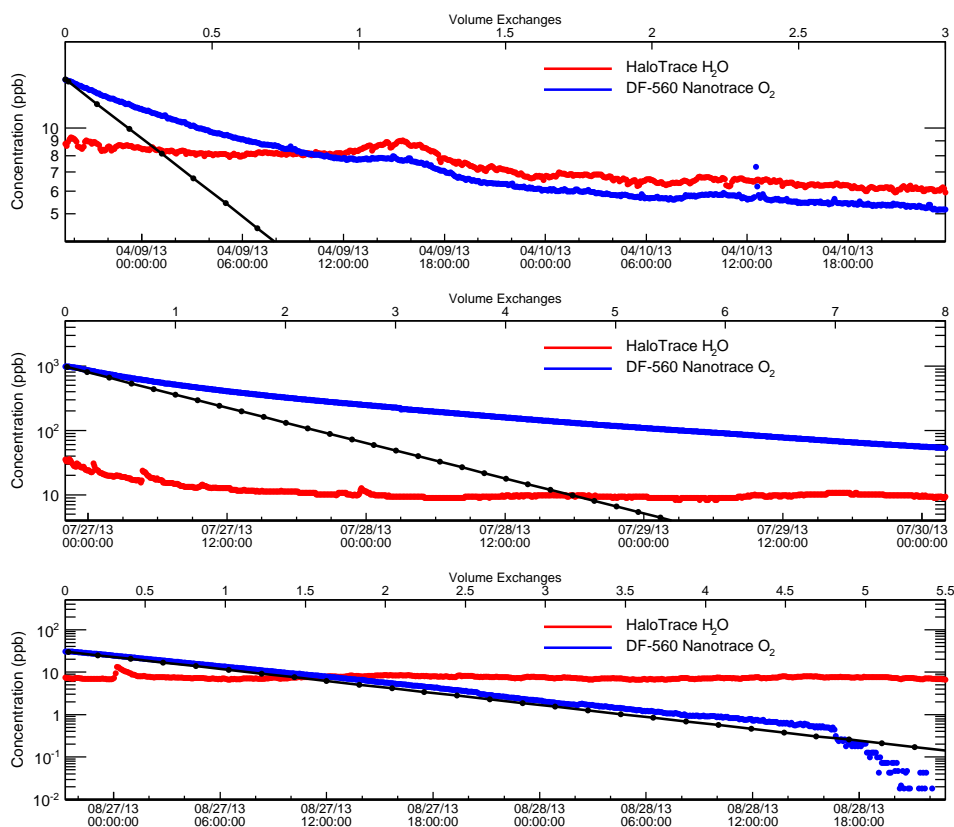


Figure 23. The water and oxygen concentrations in the cryostat liquid for three time intervals before purity monitor operation. The measured oxygen concentration (blue line) is compared to a simulation assuming perfect mixing (black line).

11 not achieved. This suggests that **what?**. However, in the last time interval, perfect mixing was
 1 **nearly** achieved.

2 Figure 24 shows the water and oxygen concentrations measured in the cryostat vapor space
 3 with the cryostat totally filled with LAr, along with the temperature in the LAPD hall. The
 4 temperature and the water concentration in the cryostat vapor space are closely correlated.
 5 **Need to finish this story.**

6 After several liquid volume exchanges, the contamination was sufficiently low to begin opera-
 7 tion of the four purity monitors inside the cryostat and the inline purity monitor upstream from
 8 the filters. The signal attenuation is defined as $1 - Q_A/Q_C$, where Q_A and Q_C are the anode
 9 and cathode peak pulse heights, respectively. The pump speed, and thus the volume exchange
 10 rate were changed over several time intervals to determine if this affected the lifetime. Figure 25
 11 shows the attenuation and pump speed over the **full range of running. I think we should break**
 12 **this up, probably at least into the regions where we achieved a good cleanup** . Needs more
 13 discussion.

14 Figure 26 shows a period of time when the LAPD experienced a pump failure. This figure
 15 also shows the water concentration in the molecular sieve. **Needs more discussion if we want to**

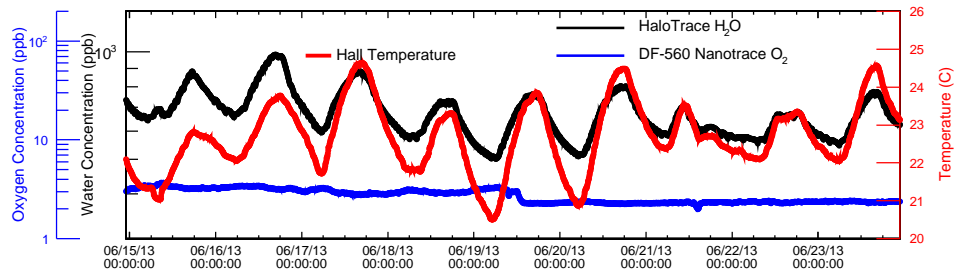


Figure 24. The water and oxygen concentrations measured in the cryostat vapor space with the cryostat totally filled with LAr. Also shown is the temperature in the LAPD hall for the same time period.

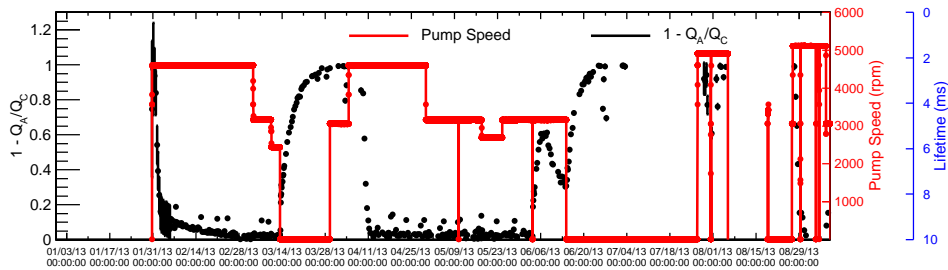


Figure 25. The attenuation ($1 - Q_A/Q_C$) for recirculated liquid argon over all LAPD running. The attenuation is correlated with electron lifetime, also shown on the right-hand scale. NOTE: This is old data that needs the few percent correction. Also shown is the pump speed.

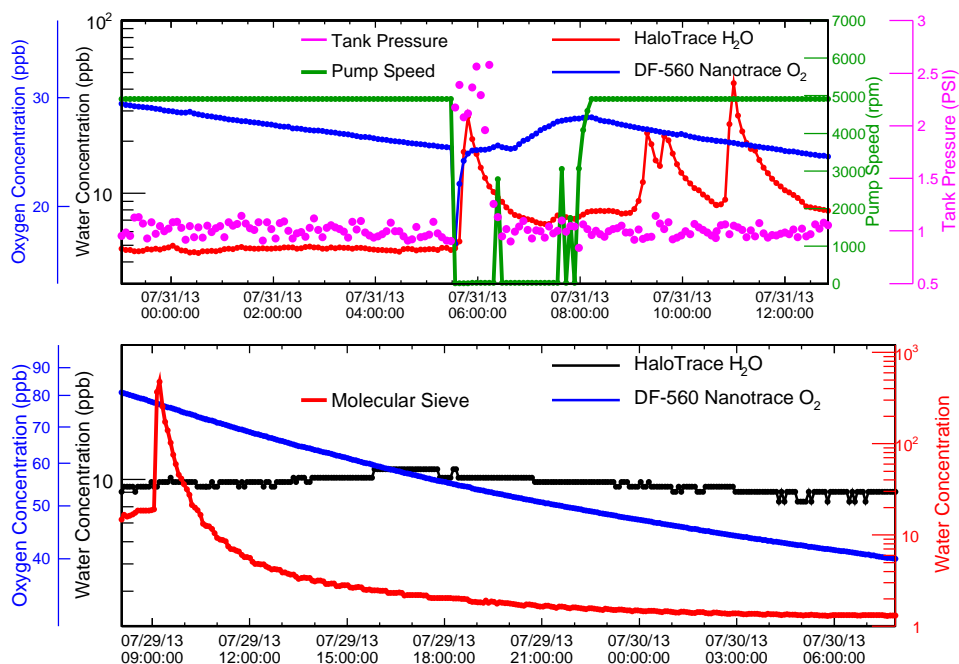


Figure 26. Top: The cryostat pressure, pump speed, and the oxygen and water concentrations in the cryostat liquid during an event when the pump was briefly turned off. Bottom: The oxygen and water concentrations measured in the cryostat liquid compared to the water concentration measured in the molecular sieve over the same time period. Cryostat cleanup drastically falls behind cleanup in the molecular sieve, etc.

16 include this.

1 6. Discussion and Conclusion

2 **This needs some work.** The primary goal of the Liquid Argon Purity Demonstrator (LAPD)
 3 has been achieved. The required level of purity can be achieved in a large volume of liquid argon
 4 without first evacuating the vessel containing the liquid and LArTPC. This test is motivated by
 5 the desire to obviate costs associated with the construction of an evacuable cryostat for future
 6 multi-kiloton detectors.

7 In addition to showing that evacuation is not necessary for achieving long electron lifetimes,
 8 we studied temperature gradients, liquid argon volume exchanges, filter capacity, and the effect
 9 of other materials. **Discuss each of these.** The results demonstrated that the technique works in
 10 the presence of material and nominal electron drift lifetimes were recovered after **X** minutes.

11 Indications from the MTS suggest the water concentration increases as the sample temperature
 12 increases, and the electron lifetime decreases. This demonstrates two major findings from the
 13 MTS. First, there is a direct relationship between electron lifetime and water concentration.
 14 Second, the water concentration does not change when materials are submerged in the liquid,
 15 but it does increase when materials are in the vapor space. Attention was given to how one
 16 would scale the system for kiloton scale masses of liquid argon and the potential scaling of the
 17 cost for such large systems.

18 Acknowledgments

1

2 We thank the staff at FNAL for their technical assistance in running the LAPD experiment. We
3 acknowledge support by the Grants Agencies of the DOE.

4 **REFERENCES**

- 5 1. T. Akiri *et al.* (LBNE Collaboration), arXiv:1110.6249 [hep-ex].
- 6 2. S. Amerio *et al.* (ICARUS Collaboration), Nucl. Instrum. Meth. A **527**, 329 (2004).
- 7 3. C. Rubbia, *et al.* (ICARUS Collaboration), Journal of Instrumentation, **6** P07011 (2011).
- 8 4. R. Andrews, W. Jaskierny, H. Jostlein, C. Kendziora, S. Pordes and T. Tope, Nucl. Instrum.
9 Meth. A **608**, 251 (2009).
- 10 5. W. Jaskierny, H. Jostlein, S. H. Pordes, P. A. Rapidis and T. Tope, FERMILAB-TM-2384-E.
- 11 6. C. Anderson, *et al.* (ArgoNeuT Collaboration), Journal of Instrumentation, **7**, P10019
12 (2012).
- 13 7. A. Ereditato, *et al.*, Journal of Instrumentation, **8**, P7002 (2013).
- 14 8. B. Rebel, M. Adamowski, W. Jaskierny, H. Jostlein, C. Kendziora, R. Plunkett, S. Pordes
15 and R. Schmitt, T. Tope and T. Yang, J. Phys. Conf. Ser. **308**, 012023 (2011).
- 16 9. G. Carugno, B. Dainese, F. Pietropaolo and F. Ptohos, Nucl. Instrum. Meth. A **292**, 580
17 (1990).
- 18 10. O. Bunneman, B. Cranshaw and J.A. Harvey, Can J. Res. **27**, 191 (1949)
- 19 11. E. Voirin, LAPD Cryostat Interior temperatures-RTD measurements and CFD models of
20 Liquid and Gas Temperatures, LARTPC-doc-635-v4, 5/13/2013